Journal of Mathematical Chemistry Vol. 37, No. 4, May 2005 (© 2005)
DOI: 10.1007/s10910-004-1105-0

A quantum theory of chemical processes and reaction rates based on diabatic electronic functions coupled in an external field

Gustavo A. Arteca*

Département de Chimie et Biochimie, Laurentian University, Ramsey Lake Road, Sudbury, Ontario, Canada P3E 2C6 and Department of Physical Chemistry, Uppsala University, Box 579, S-751 23 Uppsala, Sweden

E-mail: Gustavo@laurentian.ca

O. Tapia

Department of Physical Chemistry, Uppsala University, Box 579, S-751 23 Uppsala, Sweden

Received 4 September 2004, revised 16 September 2004

The method discussed in this work provides a theoretical framework where simple chemical reactions resemble any other standard quantum process, i.e., a transition in quantum state mediated by the electromagnetic field. In our approach, quantum states are represented as a superposition of electronic diabatic basis functions, whose amplitudes can be modulated by the field and by the external control of nuclear configurations. Using a one-dimensional three-state model system, we show how chemical structure and dynamics can be represented in terms of these control parameters, and propose an algorithm to compute the reaction probabilities. Our analysis of effective energy barriers generalizes previous ideas on structural similarity between reactant, and product, and transition states using the geometry of conventional reaction paths. In the present context, exceptions to empirical rules such as the Hammond postulate appear as effects induced by the environment that supplies the external field acting on the quantum system.

KEY WORDS: diabatic functions, reaction rates, transition states, quantum states, external fields

1. Introduction

Experiments on single molecules show that external manipulation can influence the preferred pathway of a chemical reaction [1]. In particular, the electric field associated with the tip of a scanning–tunneling microscopy (STM) can be used to excite selectively a single adsorbate [2] and induce translation or

* Corresponding author.

desorption [3], as well as control the formation of a new product after fragmentation [4]. Electron transfer in the STM field can also become so strongly coupled to high-frequency oscillations in a single-molecule transistor [5] that one could also regard the result as a quantum process triggered by centre-of-mass motions. Similarly, growing evidence suggests that processes such as enzymatically-catalyzed proton transfers are strongly affected, and regulated, by the geometry and dynamics of the enzyme (cf. ref. 6 and others therein). These examples indicate that, in principle, it is possible to *prepare* (and control) a molecular system *externally* in such a way as to *elicit* its electronic reorganization. In particular, a sharp change in electronic quantum state can occur within certain regions of the nuclear configurational space, under the mediation of an external field. Here, we discuss a formalism to describe these phenomena and locate "reactive" configurations that can be reached by external manipulation or intrinsic activations. In our approach, quantum states are represented within a generalized electronic diabatic (GED) basis set for the interacting electron gas model; by construction, these states are *diabatic* in the sense of being independent of the geometry for the background of external positive charges (e.g., the nuclear charges). Depending on symmetry, changes in quantum state may require not only the external field but also a *diabatic transition state*. The formalism goes beyond the standard Born–Oppenheimer (BO) electronuclear separation [7]. Below, we discuss the foundations of the methodology; emphasis is made on the basic concepts required to build a model of a chemical reaction as a full quantum process, i.e., one where quantum states change amplitudes when represented as a linear superposition over the GED basis. As illustration, we apply the ideas to a simple three-state model where reaction probabilities are affected by controlling externally the geometry of the positive charge background.

2. Quantum/classical model

The key ideas of the GED approach are summarized here. In a quantum-mechanical (non-relativistic) context, a molecular system is represented by a Coulomb hamiltonian operator $\mathrm{H}_{\mathrm{mol}}(\mathbf{q},\mathbf{R};[\mathbf{Z},\mathbf{M}])$, whose eigenstates $\Psi(\mathbf{q},\mathbf{R})$ belong to an electronuclear Hilbert space supported by the vector space $\Re^{3n}\times\Re^{3m}$ associated with n-electron coordinates $\mathbf{q}$ and m-nuclei coordinates $\mathbf{R}$. The notation $\mathrm{H}_{\mathrm{mol}}(\mathbf{q},\mathbf{R};[\mathbf{Z},\mathbf{M}])$ indicates that the operator depends parametrically on the vectors $\mathbf{Z}$ and $\mathbf{M}$ representing m-nuclear charges and masses, where

$$H_{\mathrm{mol}}(\mathbf{q},\mathbf{R};[\mathbf{Z},\mathbf{M}]) = T_{\mathrm{N}}(\mathbf{R};[\mathbf{M}]) + T_{\mathrm{e}}(\mathbf{q}) + V_{\mathrm{ee}}(\mathbf{q}) + V_{\mathrm{Ne}}(\mathbf{q},\mathbf{R};[\mathbf{Z}]) + V_{\mathrm{NN}}(\mathbf{R};[\mathbf{Z}]) \tag{1}$$

with T_{N} and T_{e} the usual kinetic energy operators and V_{ee}, V_{Ne}, and V_{NN} the potential energy operators for the electron–electron, electron–nuclei, and

nuclei–nuclei interactions. The eigenfunctions of (1) form a *continuum*. As discussed by Sutcliffe [8], these wave functions can always be written as $\Psi(\mathbf{q},\mathbf{R}) = \psi(\mathbf{q},\mathbf{R})\mathrm{F}(\mathbf{R})$, but the resulting ψ and F functions are *not* eigenfunctions of any molecular hamiltonian, thus cannot be assigned a clear physical meaning. In other words, although one can always "separate" nuclei and electrons because they are *different* particles, this difference does not translate into distinct wave functions. In the BO scheme, $\psi(\mathbf{q},\mathbf{R})$ is assumed to be an eigenfunction of the nuclear-mass-independent operator $\mathrm{H_{elec}} = T_e(\mathbf{q}) + V_{ee}(\mathbf{q}) + V_{Ne}(\mathbf{q},\mathbf{R};[\mathbf{Z}])$ [7a]. The so-called "clamped-nuclei approximation" is a further simplification that introduces infinite-mass nuclei and a continuous parametric dependence of $\psi(\mathbf{q},\mathbf{R})$ (and its energy E) with the **R**-coordinates [8]. This approach has been subject to numerous criticisms and the BO potential energy hypersurface $E(\mathbf{R})$ is physically lacking on several grounds [8–11]. For the present work, the principal weaknesses are: (i) the coordinates **R** cannot be interpreted as nuclear positions when using a rotating body-fixed coordinate system with origin at the system's centre of mass [7b], (ii) chemical reactions are described as a result of unphysical continuous changes of the electronic basis functions on the single energy surface for an isolated molecular system, and (iii) the method cannot account for the fact that some low-energy reaction channels are apparently influenced by high-energy states [9,10]. Note that point (i) is important yet, unfortunately, seldom recognized as intrinsic to the BO approach.

The GED approach addresses these issues by introducing a *de facto* separation between quantum particles (the electrons) and a set of *classical positive test charges*. In a first approach, the masses of the latter particles (e.g., the nuclei) do not enter into the description. The resulting quantum/classical hamiltonian $\mathrm{H_{Q/C}}$ depends on the n-electron **q**-coordinates and the $\boldsymbol{\xi}$-coordinates for the configuration of positive charges, yet has no information on nuclear masses

$$\mathrm{H_{Q/C}}(\mathbf{q};[\boldsymbol{\xi},\mathbf{Z}]) = T(\mathbf{q}) + V(\mathbf{q};[\boldsymbol{\xi},\mathbf{Z}]) = T(\mathbf{q}) + V_{ee}(\mathbf{q}) + V_{Ne}(\mathbf{q};[\boldsymbol{\xi},\mathbf{Z}]) + V_C([\boldsymbol{\xi},\mathbf{Z}]). \tag{2}$$

The potential $V_C([\boldsymbol{\xi},\mathbf{Z}])$ is the interaction between classical charges; $V_{Ne} + V_C$ is an "external" potential acting on the n-electron system. In a model with classical charges, the $\boldsymbol{\xi}$-configurations can be manipulated *externally* at will, and thus the $\mathrm{H_{Q/C}}$ hamiltonian depends parametrically on the latter (but not the basis functions). Both the operator $\mathrm{H_{Q/C}}$ and its eigenstates are described with inertial (nonrotating) frames; velocities and translational energies for reactant states introduce only phase factors in the wave functions [12].

When $\mathbf{Z} = \mathbf{0}$, $\mathrm{H_{Q/C}}$ represents n-interacting electrons and its eigenstates span a $\boldsymbol{\xi}$-*independent* continuum. Our central idea is that the eigenfunctions of $\mathrm{H_{Q/C}}(\mathbf{q};[\boldsymbol{\xi},\mathbf{0}])$ form a complete ensemble and contain all the information (including electron correlation) needed to describe the quantum states of *any* n-electron system consistent with a given **Z**-vector. In the context of the present

quantum/classical hamiltonian $H_{Q/C}$, it is worth restating two important results for electron and nuclear operators due to Kato [13]

(1) The domain D_H of the hamiltonian $H(\mathbf{q}) = T(\mathbf{q}) + V(\mathbf{q})$ is that of $T(\mathbf{q})$, the (purely kinetic) hamiltonian for free electrons, for any V potential satisfying: $\|V\phi\| \leqslant a|T\phi\| + b\|\phi\|$, for every $\phi \in D_H$ and two constants a and b, where $\|A\phi\|^2 = \langle A\phi|A\phi\rangle_{(\mathbf{q})}$. As discussed in ref. 13, this theorem is valid for *any* Coulomb operator V. For our present needs, this result indicates that the domain of the hamiltonian is not affected by $\mathbf{Z}$, i.e. it is the same whether V is the full operator $V_{ee}(\mathbf{q}) + V_{Ne}(\mathbf{q}; [\boldsymbol{\xi}, \mathbf{Z}]) + V_C([\boldsymbol{\xi}, \mathbf{Z}])$ in equation (2) or $V(\mathbf{q}; [\boldsymbol{\xi}, \mathbf{0}]) = V_{ee}(\mathbf{q})$, the electron–electron repulsion.

(2) In addition to the above invariance of the hamiltonian domains D_H, we take into account that a nonrelativistic hamiltonian for a finite set of particles interacting with each other through a Coulomb potential energy is *essentially self-adjoint*. This result also applies to the model operator $H_{Q/C}(\mathbf{q}; [\boldsymbol{\xi}, \mathbf{Z}])$, even after we add spin–orbit interactions. In this theorem, essential self-adjointness implies that the spectrum of (discrete or continuous) eigenfunctions $H_{Q/C}(\mathbf{q}; [\boldsymbol{\xi}, \mathbf{Z}])$ is *complete*, although this may not be true if the V potential becomes non-Coulombic [13].

Note that result (2) indicates that the eigenfunctions of $H_{Q/C}(\mathbf{q}; [\boldsymbol{\xi}, \mathbf{Z}])$ are sufficient to represent the general quantum states of an isolated n-electron system, whereas the result (1) ensures that this set of functions is contained within the domain of the electron-only system $H_{Q/C}(\mathbf{q}; [\boldsymbol{\xi}, \mathbf{0}])$. These functions span a continuum, yet remain a complete representation for a n-electron system *nonisolated* in the presence of a external electromagnetic field, even if in these cases the standard perturbative approaches become asymptotically divergent [14].

By construction, the $\{\psi_k(\mathbf{q})\}$-eigenfunctions of $H_{Q/C}(\mathbf{q}; [\boldsymbol{\xi}, \mathbf{0}])$ contain no information on the location of the classical charges. Based on the result above, we propose to view the $\{\psi_k(\mathbf{q})\}$-eigenfunctions of $H_{Q/C}(\mathbf{q}; [\boldsymbol{\xi}, \mathbf{Z}])$ as a complete set of *diabatic* basis functions, i.e., independent of the $\boldsymbol{\xi}$-geometry of the background of classical charges for any given $\mathbf{Z}$-vector. It should be pointed out that these "formal diabatic basis functions" are *not* built as linear combinations of adiabatic functions derived from the BO approach, as done in the numerous schemes available for deriving quasi-diabatic functions [9,11,15–25]; indeed, such combinations are *not*, in general, globally diabatic [16,18,23], although they remain a useful tool in regions of configurational space, depending on the nature of the residual nonadiabatic coupling terms (NACTs) associated with the nuclear gradient operator [25]. As discussed below, functions computed at specific stationary $\boldsymbol{\xi}$-geometries can also be used as a first approximation to the $\{\psi_k(\mathbf{q})\}$-eigenfunctions introduced in the GED approach. The central difference is the nature of their coupling: whereas quasi-diabatic functions are coupled

through by NACTs, we focus presently in the coupling through an external field. The latter feature remains a factor even if one neglects all nuclear-coordinate derivatives.

In the present approach, each $\psi_k(\mathbf{q})$-function represents a basis state for an isolated molecular system and it is associated with a *diabatic potential energy function* defined as

$$U_k(\boldsymbol{\xi}) = \langle \psi_k(\mathbf{q}) | \mathrm{H}_{\mathrm{Q/C}}(\mathbf{q}; [\boldsymbol{\xi}, \mathbf{Z}]) \psi_k(\mathbf{q}) \rangle, \tag{3}$$

where brackets indicate integrals over $\mathbf{q}$. The $\{\mathrm{U}_k(\boldsymbol{\xi})\}$-functions represent the eigenvalues of the quantum/classical hamiltonian at the local $\boldsymbol{\xi}$-configuration (a "single-point" hamiltonian); since the $\{\psi_k(\mathbf{q})\}$-functions are diabatic, the $\{\mathrm{U}_k(\boldsymbol{\xi})\}$-eigenvalues depend on $\boldsymbol{\xi}$ only through $(V_{\mathrm{Ne}}(\mathbf{q}; [\boldsymbol{\xi}, \mathbf{Z}]) + V_{\mathrm{C}}([\boldsymbol{\xi}, \mathbf{Z}])$ in equation (2). Note that, in this context, all $\mathrm{H}_{\mathrm{Q/C}}(\mathbf{q}; [\boldsymbol{\xi}, \mathbf{Z}])$ operators share the $\{\psi_k(\mathbf{q})\}$-eigenfunctions, but *not* necessarily with the same eigenvalues. Except at isolated $\boldsymbol{\xi}$-configurations, the $\{\psi_k(\mathbf{q})\}$-functions are nondegenerate, i.e. $\langle \psi_k(\mathbf{q}) | \psi_j(\mathbf{q}) \rangle = \delta_{kj}$. From this, we deduce: $\langle \psi_k(\mathbf{q}) | \mathrm{H}_{\mathrm{Q/C}}(\mathbf{q}; [\boldsymbol{\xi}, \mathbf{Z}]) \psi_j(\mathbf{q}) \rangle = 0$, for all $\boldsymbol{\xi}$, if $k \neq j$. Note that, in contrast with the BO approach, there are no discontinuities in the $\{\psi_k(\mathbf{q})\}$-functions or their derivatives whenever two potential energy functions $\{\mathrm{U}_k(\boldsymbol{\xi})\}$ cross.

Since $\psi_k(\mathbf{q})$ do not depend on $\boldsymbol{\xi}$, the matrix element $\langle \psi_k | \mathrm{H}_{\mathrm{Q/C}} \psi_j \rangle$ will vanish for $k \neq j$ for any $\boldsymbol{\xi}$, even if the $\{\psi_k(\mathbf{q})\}$-functions have been calculated at a configuration $\boldsymbol{\xi}' \neq \boldsymbol{\xi}$. Note that this is a property of the diabatic *exact* basis functions; approximate solutions (e.g., Hartree–Fock wave functions or their extensions involving some electron-correlation effects) do not satisfy this property globally over the entire $\boldsymbol{\xi}$-space.

The existence of a complete basis of $\{\psi_k(\mathbf{q})\}$-functions does not provide information about the spectrum, beyond it being bounded from below and unbounded from above [13]. In particular, not all $\psi(\mathbf{q})$ functions need be consistent with a molecular *bound* state; some of these state may be represented by specific linear combinations of the latter. Therefore, we introduce the notion of *chemical species* by associating each to a single-minimum diabatic potential attractor with the following two requirements:

(1) A *diabatic* $|\psi_k(\mathbf{q})\rangle$-basis state for an isolated n-electron *molecular* system satisfies the stationary solutions $\partial \mathrm{U}_k(\boldsymbol{\xi})/\partial \mathbf{Z}|\mathbf{Z}^* = 0$ and $\partial \mathrm{U}_k(\boldsymbol{\xi})/\partial \boldsymbol{\xi}|_{\boldsymbol{\xi}^{(k)}} = 0$ [26].

(2) A bound $|\psi_k(\mathbf{q})\rangle$-basis state defines a potential energy attractor $\mathrm{U}_k(\boldsymbol{\xi})$ with *only one* minimum-energy stationary geometry, denoted by $\boldsymbol{\xi}^{(k)}$. These $\boldsymbol{\xi}^{(k)}$-geometries will correspond to asymptotic attractors in the case of $|\psi_k(\mathbf{q})\rangle$-states representing separate molecular fragments [12].

The integer solutions $\mathbf{Z}^*$ corresponds to chemical systems that can be achieved with realistic charges. These $\mathbf{Z}$-systems admit a number of bound

chemical species, each of which is associated with a *single-minimum potential energy attractor*. Each molecular $U_k(\boldsymbol{\xi})$-attractor is a confining function with respect to the limit of the electron-only gas ($\mathbf{Z}=\mathbf{0}$). These species can be given arbitrary $\boldsymbol{\xi}$-configurations and yet remain at the same $|\psi_k(\mathbf{q})\rangle$-state. Our contention now is that *nonisolated* systems *can change* the electronic quantum state depending on the local $\boldsymbol{\xi}$-geometry imposed. As long as an external field couples a subset of relevant $|\psi_k(\mathbf{q})\rangle$-basis states, it would be possible to build a minimalist model of a reaction process evolving as a change in general quantum state.

3. Electronic processes in laboratory space

Using the results in the previous section, consider a nonisolated system that interacts with an external field; the total hamiltonian H_{tot} can be written in the first (dipolar) approximation as [12]

$$H_{tot}(\mathbf{q}) = H_{Q/C}(\mathbf{q};[\boldsymbol{\xi},\mathbf{Z}]) + V_{field} \approx H_{Q/C}(\mathbf{q};[\boldsymbol{\xi},\mathbf{Z}]) - (e/mc)\mathbf{A}\cdot\mathbf{p}, \tag{4}$$

where $\mathbf{A}$ is the electromagnetic vector field and $\mathbf{p}$ the electronic total linear momentum operators (both represented using the same inertial frame). Invoking the completeness of the diabatic basis set, we represent the eigenstates $\{|\Phi\rangle\}$ of H_{tot} as a linear superposition in the eigenfunctions of $H_{Q/C}(\mathbf{q};[\boldsymbol{\xi},\mathbf{Z}])$, where the linear combination coefficients $c_s(\boldsymbol{\xi};\mathbf{A})$ depend parametrically on the applied field and contain all the information of the local $\boldsymbol{\xi}$-geometry for the classical charges

$$\Phi(\mathbf{q};[\boldsymbol{\xi}]) = \sum_s c_s(\boldsymbol{\xi};\mathbf{A})\psi_s(\mathbf{q}) = (c_1(\boldsymbol{\xi}),\ldots,c_i(\boldsymbol{\xi}),\ldots)[\psi_1(\mathbf{q}),\ldots,\psi_i(\mathbf{q}),\ldots]. \tag{5}$$

A quantum state $|\Phi\rangle$ is simply defined by the coefficient vector $\mathbf{c}(\boldsymbol{\xi}) = (c_1(\boldsymbol{\xi}),\ldots,c_i(\boldsymbol{\xi}),\ldots)$ in the infinite Hilbert space of diabatic functions; changes in quantum state correspond to shifts in this vector. However, when applying equation (5) in practice, one must take into account that studying a system in the laboratory introduces constraints in the form of boundary conditions and windows of accessible energies. These constraints translate into the fact that only a *finite subset* amplitudes in the diabatic basis functions, $\{\psi_k, k=1,2,\ldots,M\}$, may be needed to account for all relevant observations. From the viewpoint of externally manipulating the classical $\boldsymbol{\xi}$-configurations, each $(0,\ldots,0,c_k(\boldsymbol{\xi})\approx 1,0,\ldots)$-state in this subset would correspond to one possible way of preparing the isolated molecular system in laboratory space. However, since "preparing" a quantum system implies that it is nonisolated, it is *not* possible to achieve a purely diabatic quantum state, e.g. $\mathbf{c}(\boldsymbol{\xi}) = (0,\ldots,0,c_i=1,0,\ldots,c_M=0)$. Even if we approach closely a condition $|\Phi\rangle \approx c_i|\psi_i\rangle, c_i \approx 1$, other states in the linear combination (5) are always present. These "residual" contributions are essential if the general

quantum state is to evolve physically among diabatic states *for different* $\boldsymbol{\xi}$*-configurations*. For this reason, the choice of the finite set $\{\psi_k, k = 1, 2, \ldots, M\}$ must be careful. To this end, we introduce another notion:

Definition 1. The finite basis subset $\{\psi_k, k = 1, 2, \ldots, M\}$ contains two classes of states. Class 1 includes all possible reactant/product states that can be prepared in laboratory space with energies consistent with observations and an accessible region of $\boldsymbol{\xi}$-configurations. Class 2 contains those excited states required for describing the electronic-transition mechanisms occurring in a region of $\boldsymbol{\xi}$-space that overlaps the one corresponding to the reactant/product states in Class 1.

As an illustration, definition 1 will imply that if we want to describe the quantum states for a system initially prepared as a classical H+H collision, we must include not only a selection of relevant diabatic states for two hydrogen atoms, but also those for other possible experiments on the two-electron system, e.g., $H^- + H^+$ or $e^- + H_2^+$ collisions (in addition to the H_2 molecule). Alternatively, one could represent the quantum states by using the set of *all* possible direct products between two hydrogen-atom wave functions (including discrete and continuum states). These diabatic states may be coupled in an external field. Ultimately, the choice of the minimum set of M diabatic functions will be dictated by how the system is studied (or prepared) in the laboratory. Often, describing some observables (e.g., a rate constant for a given reaction channel) requires that we include high-energy diabatic states with prescribed symmetries in Class 2; these states may or may not correlate with asymptotic states. Some known failures of the BO scheme can be traced indeed to the fact that some relevant high-energy states are left out of the analysis [9].

Whereas the superposition (5) is sensible for the eigenfunctions of the total operator $H_{\mathrm{tot}}(\mathbf{q})$, there is no guarantee that the spectrum of $H(\mathbf{q}, \boldsymbol{\xi})$ (with $U_k(\boldsymbol{\xi})$ eigenvalues) is sufficient to represent the $\Phi(\mathbf{q}, \boldsymbol{\xi})$-eigenfunctions for the full molecular hamiltonian including quantum nuclear states. This issue can be addressed by an *additional* requirement, whereby equation (5) is also used to represent $\Psi(\mathbf{q}, \boldsymbol{\xi})$; here, the $c_s(\boldsymbol{\xi})$-coefficients emerge as eigenfunctions of the operator $H_{\mathrm{N}} = T_{\mathrm{N}}(\boldsymbol{\xi}) + U_k(\boldsymbol{\xi})$ for the nuclear dynamics [26]. This extension is implicitly assumed but for our present needs we omit it, since the $\boldsymbol{\xi}$-configurations are considered for the moment to be manipulated *externally,* rather than by the intrinsic nuclear dynamics.

The above ideas are sufficient to build a theoretical framework where a chemical reaction resembles other quantum processes (e.g., an electronic "excitation"). In other words, a chemical process involves a change of quantum (electronic) state mediated by the electromagnetic field, and possibly influenced by an external manipulation of the nuclear configurational space.

A practical implementation of these ideas requires the choice of a convenient subset of GED functions $\{\psi_k, k = 1, 2, \ldots, M\}$. A simple choice can be

based on a series of isolated adiabatic calculations, each at the minimum-energy configuration for an attractor associated with a relevant chemical species. At each of these $\boldsymbol{\xi}^{(k)}$-geometries, with $\partial U_k(\boldsymbol{\xi})/\partial \boldsymbol{\xi} = 0$ at $\boldsymbol{\xi}^{(k)}$, we generate one of the ψ_k-functions, and then use it to construct the diabatic potential energy $U_k(\boldsymbol{\xi}) = \langle \psi_k | H_{Q/C} \psi_k \rangle$, *where* ψ_k *remains unchanged from the form evaluated at* $\boldsymbol{\xi}^{(k)}$. In this manner, each ψ_k-function would preserve the symmetries that characterize the electronic states in question (e.g., the number and symmetry of the nodal planes). When using the standard representation for ψ_k with atomic orbitals, care must be taken to ensure that orbitals located at different points in space (e.g., on a nucleus) are consistent with the laboratory frame. Further information could be introduced into the model by fitting the approximate diabatic potential energy curves to "cross" at known conical intersections [25]. This procedure would increase the quality of a finite set of GED functions, while avoiding the drawbacks associated with the residual nuclear-coordinate dependence that characterize quasi-diabatic functions [14–25, 27]. Below, we illustrate these notions in a simple model for the isomerization of two closed-shell species (e.g., a keto→enol reaction). In the simplest case, the external field may be a monochrome laser beam.

4. Chemical reactions and rate constants in a three-state model system

4.1. *Effective potential energy functions*

For illustration, consider two chemical species whose electronic structures are described by the diabatic basis functions $\psi_1(\mathbf{q})$ and $\psi_2(\mathbf{q})$ (reactant and product, respectively). These could correspond to a keto (reactant) and enol (product) species. We assume these species have *molecular* potential energy attractors, as opposed to asymptotic ones; in other words, their potential energy functions U_1 and U_2 do not describe molecular fragments and their minima are separated by a finite distance in a local inertial frame. In a typical isomerization, these species will be nondegenerate, closed-shell, and share the same parity. This symmetry implies $\langle \psi_1 | \psi_2 \rangle = 0$ and $\langle \psi_1 | H_{tot} \psi_2 \rangle = 0$ (cf. equation (4)), i.e., no transition take place even in presence of a field). A formal change of quantum state $|\Phi\rangle \approx c_1 |\psi_1\rangle \rightarrow |\Phi\rangle \approx c_2 |\psi_2\rangle$ must necessarily involve at least a *third* state in Class 2, say $|\psi_3\rangle$, with different parity; we call the latter a *diabatic transition state* (TS).

We can now compute the lowest energy level for H_{tot} using a three-state model where a general quantum state is represented as $\Phi = c_1\psi_1 + c_2\psi_2 + c_3\psi_3$. The $\{c_i\}$-coefficients are modulated by the external field and the classical-charge configuration. Using the symmetries of these states, and the properties of the matrix elements $(H_{tot})_{ij}$ (cf. section 2), the relevant secular equation is

$$\det \begin{pmatrix} U_1 - E_{\text{tot}} & 0 & V_{13} \\ 0 & U_2 - E_{\text{tot}} & V_{23} \\ V_{13} & V_{23} & U_3 - E_{\text{tot}} \end{pmatrix} = 0, \tag{6}$$

where the matrix elements for the field interaction, $V_{ij} = \langle \psi_i | \mathrm{V}_{\text{field}} \psi_j \rangle$, are also independent of $\boldsymbol{\xi}$. Our present goal is to understand the qualitative dependence of the $\{c_i\}$-coefficients on the field intensity (using V_{13} and V_{23} as control parameters) and the $\boldsymbol{\xi}$-configuration (through the diabatic potential energy functions $\{U_i\}$). For this reason, we base our analysis on model representations of the diabatic energies, instead of computing actual diabatic ψ_i-functions. We denote with Φ the eigenfunction of H_{tot} with the lowest energy eigenvalue E_{tot} in equation (8); the coefficients defining the corresponding quantum state $|\bar{\Phi}\rangle$ are computed as: $|c_1| = V_{13}c_3/|E_{\text{tot}} - U_1|$, $|c_2| = V_{23}c_3/|E_{\text{tot}} - U_2|$, and $|c_3| = \{(V_{13}/|E_{\text{tot}} - U_1|)^2 + (V_{23}/|E_{\text{tot}} - U_2|)^2 + 1\}^{-1/2}$.

For simplicity, we consider that the most relevant features of the configurational space can be captured by a single variable x, which can be thought as measuring the position of a particular classical charge with respect to the laboratory frame. In terms of this variable, we approximate the diabatic attractors as harmonic oscillators: $U_i(x) = \Delta_i + (k_i/2)(x - x_i)^2$, where x_i and Δ_i give the position and depth of the attractors, respectively. Figure 1 shows one such three-state system, where the diabatic product $|\psi_2\rangle$-state lies at higher energy than the diabatic reactant $|\psi_1\rangle$-state (with $\Delta_1 = x_1 = 0$ and $\Delta_2 = 3$, $x_2 = 3$), and the attractor for the diabatic (Class 2) $|\psi_3\rangle$-state is closer to that of the product (with $\Delta_3 = 5$, $x_3 = 2.5$). The force constants are chosen as $k_1 = k_2 = 2k_3 = 5$. Considering a typical reduced mass of $\mu \approx 10^3$ atomic units, the potential well for the reactant would admit *ca.* 90 vibrational levels up to the diabatic crossing $x_{\text{DC}} = 1.90$ (where $U_1(x_{\text{DC}}) = U_2(x_{\text{DC}}) = 4.5125$), whereas the product has *ca.* 30 levels at that point.

Within the standard BO approximation, one solves $\mathrm{H}(\mathbf{q}; [\boldsymbol{\xi}])\Phi(\mathbf{q}; \boldsymbol{\xi}) = \varepsilon(\boldsymbol{\xi})\Phi(\mathbf{q}; \boldsymbol{\xi})$, i.e., an infinite set of hamiltonians relating the minimal energy geometries of the reactant and the product. In this notation, we would have $\Phi_1(\mathbf{q}; \boldsymbol{\xi}^{(1)}) = \psi_1(\mathbf{q})$ and $\Phi_2(\mathbf{q}; \boldsymbol{\xi}^{(2)}) = \psi_2(\mathbf{q})$, as discussed in section 3 for the practical choice of the basis set. At the adiabatic crossing (i.e., the conical intersection (CI)), the BO-hamiltonian is ill-defined. If the electronic symmetries of $\Phi_1(\mathbf{q}; \boldsymbol{\xi}^{(1)})$ and $\Phi_2(\mathbf{q}; \boldsymbol{\xi}^{(2)})$ could be switched spontaneously at the CI, the potential energy curve would change continuously from reactant to products. The reaction would then proceed from $|\psi_1\rangle$ to $|\psi_2\rangle$ as a spontaneous switch (an "avoided crossing") among potential energy curves. Yet, the adiabatic hypothesis breaks down near x_{DC} and an alternative analysis method is needed (e.g., a quasi-diabatization scheme) [14–25]. In the GED approach, in contrast, the apparent transition $|\Phi\rangle \approx c_1|\psi_1\rangle \rightarrow |\Phi\rangle \approx c_2|\psi_2\rangle$ proceeds as an smooth effective reaction barrier $E_{\text{tot}}(x) = \langle \Phi | \mathrm{H}_{\text{tot}} \Phi \rangle$, *whose shape depends on the applied external field*. Figure 1 (top) shows one such barrier (indicated with thick line)

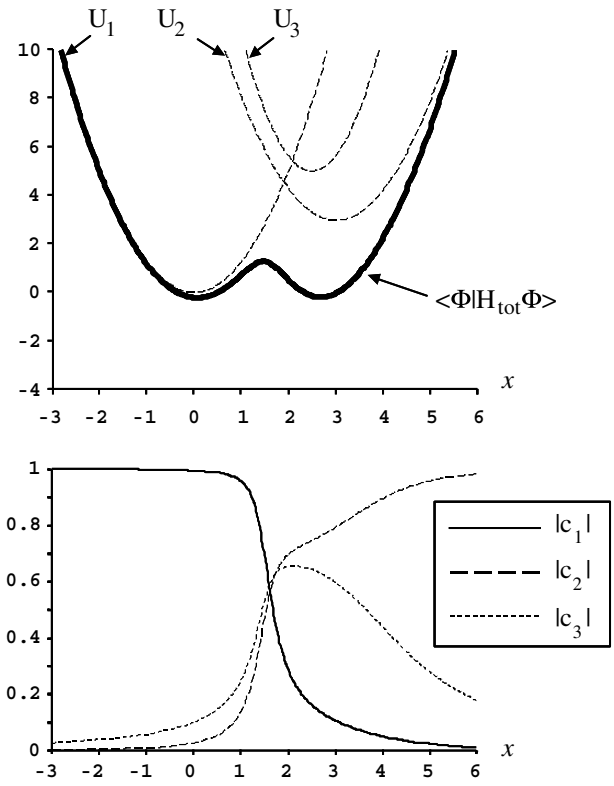

Figure 1. Double-well potential $E_{\mathrm{tot}}(x) = \langle\Phi|\mathrm{H}_{\mathrm{tot}}\Phi\rangle$ (top) and wave function coefficients (bottom) associated with the lowest energy state of a three-state model with a bound diabatic transition state (TS). The TS is more strongly coupled to the diabatic product state, $V_{23} = 2V_{13} = 4$. The TS makes the largest contribution to the total quantum state $|\Phi\rangle$ for $1.61 \leq x \leq 1.73$ decreases rapidly after the diabatic crossing $U_1 = U_3$. (See text for the potential energy functions U_i used. For the present diagrams, the configurational variable x was varied with a resolution $\Delta x = 0.01$.)

for a particular case where the diabatic product is more strongly coupled to the diabatic TS (with $V_{23} = 2V_{13} = 4$). Here, the reaction is described by an energy double well, with minima at $x_a^* = 0.06$ and $x_c^* = 2.67$, and a maximum at $x_b^* = 1.46$. The process is slightly endothermic (with $E_{\mathrm{tot}}(x_a^*) = -0.2066$ and $E_{\mathrm{tot}}(x_c^*) = -0.1851$), and the barrier height is significantly lower than the energy at the diabatic crossing ($E_{\mathrm{tot}}(x_b^*) = 1.3109$ versus $U_1(x_{\mathrm{DC}}) = 4.5125$). As a result of the stronger coupling between the Class 1 and Class 2 states $|\psi_1\rangle$ and $|\psi_3\rangle$, the position of the barrier and the effective minimum for the product (x_b^* and x_c^*, respectively) are more affected than the one corresponding to the reactant. As mentioned before, nuclear dynamics can be incorporated at this moment in the formalism.

The bottom diagram in figure 1 shows how the energy profile reflects the structure of the general quantum state $|\Phi(x)\rangle$. Some important observations can

be made: (i) Near the effective minimum for the reactant (x_a* or x_1), the quantum state resembles the diabatic reactant state, i.e. one with $\mathbf{c}(x) = (c_1, c_2, c_3)$ with $|c_1| \approx 1$, $|c_{i\neq 1}| \ll 1$. Nevertheless, the product state and TS make residual contributions that, though quite small, are essential to understand the changes in the $|\Phi(x)\rangle$-state for other x values. (ii) The diabatic reactant state remains the main contribution to $|\Phi(x) >$ for $x \leq 1.60$. Note that the effective barrier at x_b* has an associated reactant-like state, $|c_1| \approx 0.746$, $|c_2| \approx 0.434$, and $|c_3| \approx 0.505$. This would correspond to an "early transition structure" in the language of physical organic chemistry [28,29]. (iii) The diabatic TS makes the larger contribution to $|\Phi(x)\rangle$ in a narrow region ($x \in [1.61, 1.73]$), but then decreases rapidly for $x > 2.12$. The diabatic product dominates the quantum state thereafter, and reaches asymptotically $|c_2| \to 1$ for $x \gg x_c$*. (iv) The overall picture is that of a rather sharp transition around $x \approx 1.6$ from a quantum state $|\Phi\rangle$ defined by $\mathbf{c}(x < x_1) = (c_1 \approx 1, c_2 \approx 0, c_3 \approx 0)$ to a state characterized by $\mathbf{c}(x > x_2) = (c_1 \approx 0, c_2 \approx 1, c_3 \approx 0)$. The corresponding "transition configuration" is located at $x \approx 1.6$, that is much earlier than the diabatic crossing $x_{DC} = 1.9$; such a behaviour would not be found within the standard BO approach.

Since the field is constant in figure 1, a possible change in quantum state would be the result of "moving" in $\boldsymbol{\xi}$-space, as it is the case in experiments with external configurational control [1–5]. The effective energy barrier in the field is also quite different from the zero-field energy, a behaviour that also has a counterpart in experiments [3]. The barrier observed in the GED model will change with the external field and the couplings between the diabatic states (or transition moments).

Figure 2 illustrates the above idea by comparing the energy profiles for two 3-state models with different matrix elements V_{ij}. Both models have the same diabatic potential energy functions $\{U_i(x)\}$; here, the product is isoenergetic with the reactant ($\Delta_2 = 0$). In the top diagram, the product is more strongly coupled to the TS in the Class 2 subset ($V_{23} = 2V_{13} = 4$); the result is an exothermic double well with an "early" (reactant-like) barrier, consistent with the so-called Hammond rule [28]. The couplings are inverted for the bottom diagram ($2V_{23} = V_{13} = 4$), resulting in a nearly thermoneutral energy profile; the reaction barrier is displaced towards the product with respect to the top diagram. In both cases, the diabatic *reactant* state makes the largest contribution to $|\Phi(x_b^*)\rangle$, the quantum state at effective barrier. This is indicated by the shaded areas in figure 2, denoting the x-configurations where $|c_1|$ is the largest coefficient (i.e., the "reactant-like" regions). These regions, delimited by x_A and x_B, include the maximum of the effective barrier. (In both cases, there is no region on the x-axis where the diabatic TS makes the largest contribution to $|\Phi\rangle$.) Note that the reactant-like region is more expanded whenever the diabatic reactant is more strongly coupled to the TS. Here, the model would predict an effective *lower yield* of the reaction, since it becomes possible to move within a larger region of x-space (for a given energy) without triggering a transition to the product state. The chemical

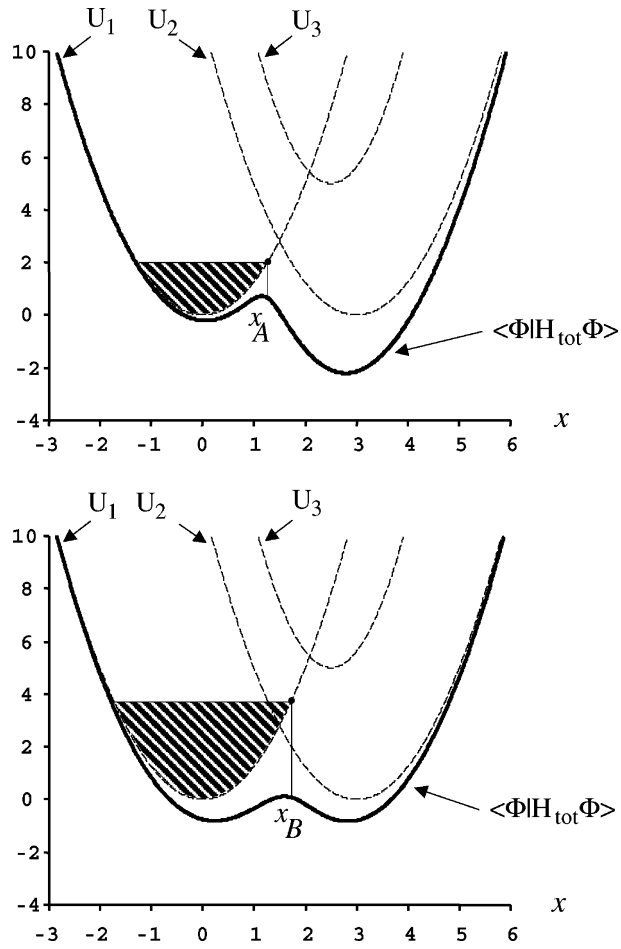

Figure 2. Regions of configurational space where the diabatic reactant state makes the main contributions to the total quantum state $|\Phi\rangle$. Both diagrams use a "product-like diabatic TS", but differ in the coupling values: $V_{23} = 2V_{13} = 4$ (top) and $V_{13} = 2V_{23} = 4$ (bottom). The points denoted by x_A and x_B represent the switch to a product-like conformation; there are no "TS-like" regions.

change requires *less energy* in the top diagram, as the configurational space for a reactant-like state is smaller: whereas the bottom diagram has *ca.* 75 vibrational levels in the reactant-like region, the number is reduced to *ca.* 40 in the top diagram. In comparison, there are *ca.* 56 levels below $U_1(x_{DC})$ at zero field. As a result, the reaction would proceed in the top diagram with energies *below* that for the diabatic crossing $U_1(x_{DC})$.

So far, we have shown how the effective energy profile $E_{tot}(x)$ and function $\Phi(x)$ change over the x-configurational space for a given field intensity. The behaviour might be different for other intensities, an effect that can be tested in

our model using the V_{ij} couplings. For simplicity, we restrict ourselves to the case where V_{ij} vary, yet the couplings' ratio remains $V_{23}/V_{13} = 2$.

In terms of the external field, the most dramatic effect is the shift in the energy barrier and its disappearance at a critical value $V_{23}^{(c)}$. Figure 3 illustrates this behaviour for the 3-state model in figure 1 (top). The figure gives the position of the barrier in terms of $\theta = (x_b{}^* - x_a{}^*)/(x_c{}^* - x_a{}^*)$, which is the fraction of a conventional reaction path connecting the two minima in the effective energy $E_{\mathrm{tot}}(x)$. At zero-field ($V_{23} = 0$), we have $\theta = 1.9/3 \approx 0.6333$. As the coupling increases, the barrier shifts initially towards the product ($\theta > 0.6333$), but then turns towards the reactant. (Figure 1 (top) corresponds to $V_{23} = 4$ and produces a "nearly-midway" barrier with $\theta = 0.5364$.) At the critical value $V_{23}^{(c)} \approx 7.22$, the barrier disappears ($\theta = 0$). For $V_{23} > V_{23}^{(c)}$, $E_{\mathrm{tot}}(x)$ is a single well and its minimum approaches that of the diabatic TS for $V_{23} \to \infty$.

As V_{23} increases, the barrier not only shifts but also decreases in height. In addition, the $x_c{}^*$-minimum deepens, that is, the *energy profiles become exothermic* for larger V_{23} values. Figure 4 illustrates how this behaviour modifies the structure of the quantum state at the barrier, in terms of a variable $\delta = [E_{\mathrm{tot}}(x_b{}^*) - E_{\mathrm{tot}}(x_a{}^*)]/[U_1(x_{\mathrm{DC}}) - U_1(x_1)]$ measuring the barrier height relative to the energy difference at the diabatic crossing. According to figure 4, $|\Phi(x_b{}^*)\rangle$ resembles the diabatic reactant ($|c_1| > |c_2|$) once the height of the barrier is sufficiently reduced; here, this corresponds to $\delta \leqslant 0.835$, or to $V_{23} \geqslant 1.21$ in

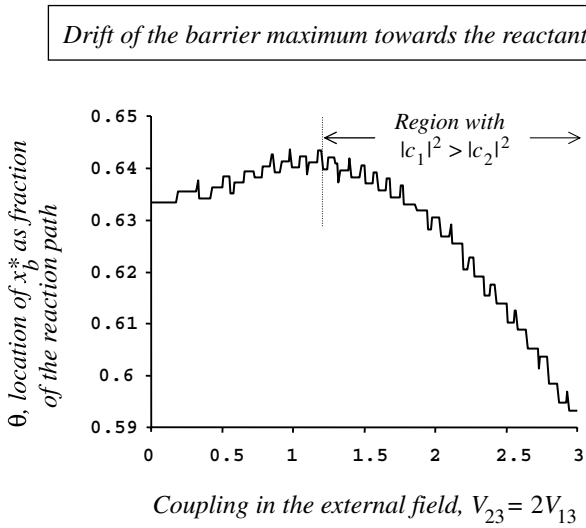

Figure 3. Drift in the location of the barrier's maximum, $E_{\mathrm{tot}}(x_b^*)$, as a function of the V_{23} coupling for the model in figure 1 (top); θ gives the location as a fraction of the path between the effective reactants and products ($x_a{}^*$ and $x_c{}^*$). The coefficient $|c_1|$ makes the largest contribution to the state $|\Phi(x_b^*)\rangle$ for $V_{23} \geqslant 1.21$; for lower V_{23} values $|c_1|$ and $|c_2|$ re-cross often. The dominance of $|c_1|$ coincides, on average, with the beginning of a systematic shift in $x_b{}^*$ towards the reactant.

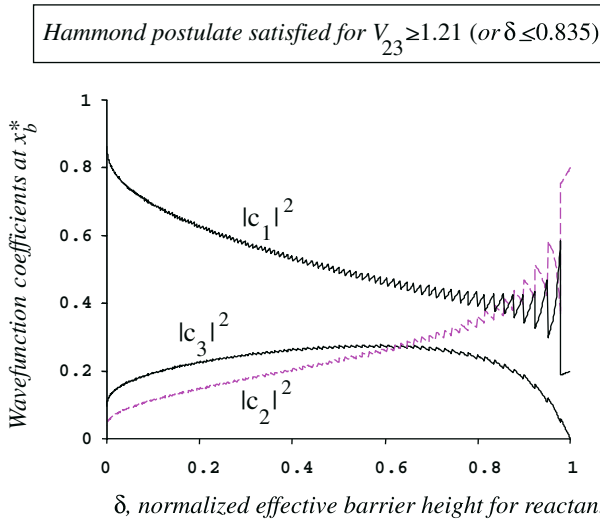

Figure 4. Amplitudes $|c_i|^2$ for the $|\Phi(x_b^*)\rangle$-state corresponding to the maximum of the effective barrier appearing in the models for figure 1 (top) and figure 3. The amplitudes are given as a function of the barrier height, normalized to the energy difference at the diabatic crossing: $\delta = [E_{\text{tot}}(x_b^*) - E_{\text{tot}}(x_a^*)]/[U_1(x_{\text{DC}}) - U_1(x_1)]$. The $|\Phi(x_b^*)\rangle -$ state becomes reactant-like ($|c_1| > |c_2|$) when the effective barrier's height is reduced ($\delta \leqslant 0.835$), as expected for exothermic double wells.

figure 3. It should be noted, however, that E_{tot} is an exothermic double well (i.e., $E_{\text{tot}}(x_c^*) < E_{\text{tot}}(x_a^*)$) *only* for $4.02 < V_{23} < V_{23}^{(c)} = 7.22$, which corresponds to $\delta < 0.3334$ in figure 4. Using our approach as a quantitative measure of similarity between the general quantum state and a diabatic state, we can make the following observations:

(i) *Exothermic* barriers have indeed "early" or "reactant-like" transition structures, consistent with the qualitative Hammond rule [29]. In the above examples, the reactant makes over a 60% contribution to the "transition structure," the latter being defined as the transient configuration for the maximum of the barrier.

(ii) There exists also a range of *endothermic* barriers with reactant-like "transition structures." These may occur at some values of the external field, and can account for known exceptions to the Hammond rule [29].

(iii) Our approach generalizes previous work seeking to measure the similarity between transition structures, reactant, and product states using distances along conventional reaction paths [28,29]. Figure 3 shows that the displacements along the reaction path are not directly correlated with linear changes in the structure of the wave function at the barrier configuration. The present similarity measure should be more

reliable given that is based on comparing quantum states, rather than configurations. Moreover, our result accommodates the case of chemical reactions which proceed along pathways that are far away from the standard (adiabatic) transition structure [30]. In the GED scheme, such reactions would reflect the fact that the general quantum state can also reach, under special conditions, a large amplitude in the diabatic product channel even at molecular geometries near that of the attractor for the diabatic reactant.

4.2. Reaction rate probabilities

As shown in section 4.1, we can use the GED approach to compute "reactive configurations", i.e., the region of x-configurational space where the diabatic *product* state dominates ($|c_2|^2 > |c_{i\neq 2}|^2$). Whether or not a system reaches these configurations depends on the energy provided externally, e.g., by a thermal bath. We can use these ideas to define the *effective reaction probability* (ERP) as an approximation to the rate constant for the process $\mathbf{c}(x < x_1) \approx (1, 0, 0) \rightarrow \mathbf{c}$ $(x > x_2) \approx (0, 1, 0)$. Note that a coefficient c_k different from zero would mean that any experiment targeting the spectrum originated at the respective diabatic basis state will show up with an intensity proportional to $|c_k|^2$.

There are several methods for the computation of reaction probabilities based on combining Newtonian or Brownian molecular dynamics with adiabatic and quasi-diabatic potential energy surfaces [31–43]. In these schemes, surface hopping and residence is controlled by the NACTs, in particular near conical intersections. In contrast, quantum-state transitions in the present GED approach relate to geometry-independent couplings with an external field. The key notion in the our method is that the external field contributes to the rate constant in two ways: (i) it establishes the limit $\boldsymbol{\xi}_{\text{lim}}$ for reactive configurations, and (ii) it provides an energy distribution which allows the system to probe the reactive configurations.

Despite the different rationale for the occurrence of a quantum-state transition, an algorithm for computing the ERPs can profit from the techniques used elsewhere for exploring the configurational space [31–43]. A simple implementation would be as follows (cf. figure 5):

(a) We first determine the set of configurations for the m-classical test charges, $\boldsymbol{\xi} \in \Re^{3m}$, where the contribution of the diabatic reactant state to the total quantum state reaches that of the product, $|c_2|^2 = |c_1|^2$. These configurations are denoted by the vector $\boldsymbol{\xi}_{\text{lim}}$; this value depends on the applied external field through the *intensity* of the vector field, A (cf. equation (4)). In the one-dimensional scheme of figure 5, this corresponds to the coordinate denoted by $x_{\text{lim}}(V_{\text{field}})$.

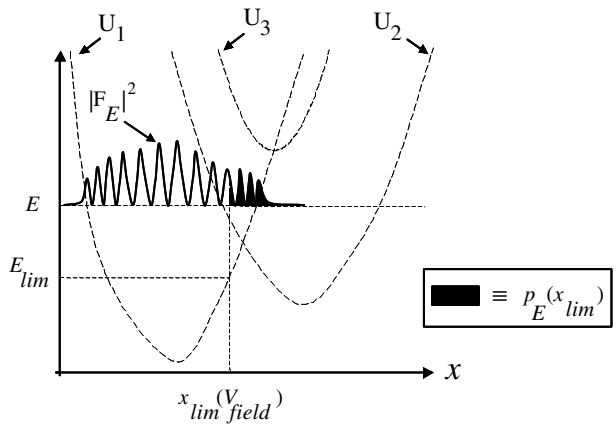

Figure 5. Scheme for the computation of effective reaction probabilities within the GED approach. The $x_{\rm lim}$-configuration limits the region where the diabatic reactant state is dominant. This configuration depends on the external field and is evaluated as in figures 1 and 2. The function $|F_E|^2$ represents the probability distribution for the nuclear motion with energy E; the shaded region $p_E(x_{\rm lim})$ gives the probability to reach "reactive" configurations (i.e., $x > x_{\rm lim}$). When computing the final reaction probabilities, E is weighed with a distribution W_E (e.g., a Maxwell–Boltzmann one) that allows the molecular system to probe regions of the configurational space.

(b) We can now define the convex hull for the limit configurations, $S_{\rm lim}$ = convex hull $\boldsymbol{\xi}_{\rm lim}$, and its interior $\Omega_{\rm lim} = {\rm int}(S_{\rm lim}) \supseteq S_{\rm lim}$. On $S_{\rm lim}$, we evaluate the minimum potential energy that the reactant needs in order to reach reactive configurations: $E_{lim} = \min U_1(\boldsymbol{\xi} \in S_{\rm lim})$. If we include nuclear dynamics, this energy will be associated with a *vibrational* energy level for the reactant.

(c) The "reactive" configurations can be defined as those where the diabatic *product* state makes the largest contribution to $|\Phi\rangle$. This set is *included* in the complement of $\Omega_{\rm lim}$, denoted by $\Omega_{\rm field}$

$$\Omega_{\rm field} = \{\boldsymbol{\xi} \in \Re^{3m} : |c_2(\boldsymbol{\xi}, A)|^2 > |c_{i\neq 2}(\boldsymbol{\xi}, A)|^2\} \subset \Re^{3m} \backslash \Omega_{\rm lim}. \tag{7}$$

Note that the $\{c_i\}$ coefficients depend on $\boldsymbol{\xi}$ and A, but not on the vibrational energy E. The set configurations (7) excludes any region where a diabatic TS might be dominant.

(d) If the external field contributes a distribution of A-values, we can define mean values for the limit configurations and also for the region with reactive configurations

$$\langle \boldsymbol{\xi}_{\rm lim} \rangle = \int_{V_{\rm field}} \boldsymbol{\xi} {\rm d}A \Big/ \int_{V_{\rm field}} {\rm d}A, \tag{8a}$$

$$\langle \Omega_{\rm field} \rangle = \int_{V_{\rm field}} \Omega_{\rm field} {\rm d}A \Big/ \int_{V_{\rm field}} {\rm d}A. \tag{8b}$$

We can now evaluate the probability of a system with energy E to reside in $\langle\Omega_{\text{field}}\rangle$.

(e) Let $\mathrm{F_E}(\boldsymbol{\xi})$ be the nuclear wave function associated with the reactant's diabatic energy, $U_1(\boldsymbol{\xi})$. This function is the solution of the Schrödinger equation for the operator $H_{\mathrm{N}} = T_{\mathrm{N}}(\boldsymbol{\xi}) + U_1(\boldsymbol{\xi})$, with eigenvalue E. Since $|\mathrm{F}_E|^2 \mathrm{d}\boldsymbol{\xi}$ represents the probability for the system to be in $\mathrm{d}\boldsymbol{\xi}$ with energy E, the probability to reside in the reactive region Ω_{field} (for a given A value) will be

$$p_E = \int_{\Omega_{\text{field}}} |F_{\mathrm{E}}|^2 \mathrm{d}\boldsymbol{\xi}. \tag{9}$$

In figuire 5, p_E is represented as a black-shaded region. Alternatively, the probability to reside in $\langle\Omega_{\text{field}}\rangle$ could be determined by an external device controlling the energy E (e.g., an STM-tip) or by stochastic search (e.g., a Monte Carlo algorithm). Below, the probability density $|\mathrm{F}_E|^2$ should be regarded in these general terms, and not only as determined by the internal nuclear dynamics.

(f) For each $\boldsymbol{\xi}$-configuration in the reactive region, the probability to generate the product response is proportional to the amplitude $|c_2(\boldsymbol{\xi}, A)|^2$. Since the probability density for the $\boldsymbol{\xi}$-configuration is $|\mathrm{F}_E|^2$ and depends on the vibrational energy E, we can estimate the reaction probability for E as

$$P(E) = \int_{\langle\Omega_{\text{field}}\rangle} |\mathrm{F}_E|^2 |c_2(\boldsymbol{\xi}, A)|^2 \mathrm{d}\boldsymbol{\xi}. \tag{10}$$

If we think in terms of sampling the $\boldsymbol{\xi}(t)$-configurations dynamically and following the amplitude $|c_2(\boldsymbol{\xi}(t), A)|^2$ for a long time until equilibrium, then the above approach will include all recrossing events leading back to the initial (reactant) state. This behaviour follows as a consequence of the conservation of the norm in the statistical ensemble average restricted to products and reactants, i.e., $\lim_{\tau\to\infty} \frac{1}{\tau} \int_0^\tau (|c_1|^2 + |c_2|^2) \mathrm{d}t = 1$. The diabatic TS $|\psi_3\rangle$ plays only the role of a "catalyst" for the quantum-state transition at *intermediate* (finite) times and disappears from the average; yet, the TS is necessary as it sustains the electronic mechanism that opens the product channel.

(g) The total ERP for the transition from reactant to product, $(\mathrm{ERP})_{R\to P}$, is the mean value of equation (10) in the energy distribution W_E provided by the radiation field

$$(\mathrm{ERP})_{R\to P} = \int_{E_{\text{lim}}}^{\infty} W_E P(E) \mathrm{d}E. \tag{11}$$

For a thermal bath with temperature T, this distribution can be described by a Maxwell–Boltzmann function $W_E \propto E^s e^{-E/kT}$, $s \geqslant 1/2$. In general, W_E is a function *controlled externally in laboratory space*. (For other ways to combine a classical bath with semiclassical quasi-diabatic dynamics, see ref. 39). The resulting reaction probability in equation (11) should be proportional to the reaction rate constant, $(\mathrm{ERP})_{R\to P} \propto k_{R\to P}$; the proportionality constant would be expected to depend on the temperature and the characteristic vibrational frequencies for the diabatic states in Class 1 used in the model.

The above algorithm is general enough to allow one to implement it in models with various numbers of diabatic states in Class 1 and Class 2, as well as different ways to map the $\boldsymbol{\xi}$-configurations in laboratory space. In particular, we can use molecular dynamics to follow the accessible $\boldsymbol{\xi}$-configurations as a function of time, as done with classical [31–35] and quantum dynamics (e.g., the END method [44]) in the context of quasi-diabatic molecular energy surfaces.

For illustration, let us consider the case of using Newtonian dynamics. In the standard methods quasi-diabatic methods, two main approaches are followed: (i) in the "surface hopping" method, a molecule is allowed to "jump" among potential energy surfaces, but the quantum-mechanical force is computed on a single energy surface at a time, and (ii) in the Ehrenfest or "mean-field" method, the molecule evolves on the weighed average of adiabatic surfaces (see ref. 45 for a comparative review). When combining the GED approach with molecular dynamics, the total force acting on the molecule should be computed from the total quantum state $|\Phi\rangle$

$$\partial^2 \boldsymbol{\xi} / \partial t^2 = -\nabla_{\boldsymbol{\xi}} E_{\mathrm{tot}}, \tag{12}$$

where $\nabla_{\boldsymbol{\xi}}$ is the nuclear coordinate gradient operator acting on the effective energy barrier associated with the current quantum state, $\mathrm{E_{tot}} = \langle \Phi | \mathrm{H_{tot}} \Phi \rangle$, for a given external field $\mathbf{A}$. The numerical solution of equation (12) will yield classical trajectories where $\boldsymbol{\xi}(t)$ evolves over time, and results in changes to the $\{c_i(\boldsymbol{\xi}; \mathbf{A})\}$-coefficients of the linear superposition in the electronic diabatic basis set. Depending on the trajectory and the $|c_i(\boldsymbol{\xi}(t); \mathbf{A})|^2$ amplitudes, it would be possible to observe transitions to products, as well as recrossing to reactants.

5. Concluding remarks

Equation (11) approximates the rate constant of the process leading from $|\Phi\rangle \approx c_1 |\psi_1\rangle$, $c_1 \approx 1$, to $|\Phi\rangle \approx c_2 |\psi_1\rangle$, $c_2 \approx 1$. It incorporates the effects of the external field through the energy distribution W_E and the accessible reactive configurational space $\langle \Omega_{\mathrm{field}} \rangle$. The GED approach also takes into account the role of a diabatic TS, or any other excited state, as key factors that modulate the value of the local reactive probability $|c_2|^2$. Indeed, the basis set of diabatic states can be expanded until one builds a satisfactory qualitative model that accounts

for $k_{R\to P}$ along a given reaction channel. In equation (11), vibrational dynamics is handled approximately by using U_1 as the (diabatic) potential energy for the nuclei in the *initial* reactant state. If the system is dressed with the electromagnetic field **A**, an improved method will require using the total energy in the field ($E_{\rm tot}$) for quantizing the nuclear motion. An even more general algorithm would consider an arbitrary (laboratory-controlled) probability function for visiting $\boldsymbol{\xi}$-configurations and a stochastic (or molecular dynamics) process to establish whether the $|c_2(\boldsymbol{\xi},A)|^2$ value is sufficiently close to unity to be able to speak of a transition to the product state. In all cases, the total quantum state will always remain *coherent*, i.e., a linear superposition in the diabatic basis for all $\boldsymbol{\xi}$-geometries. Nevertheless, equation (11) provides the basis for a theory of reaction rates that uses an electronic diabatic basis set and an external field, as opposed to the BO separation scheme and NACTs, to describe the external control of chemical processes.

Acknowledgments

This work was supported by Grants from NSERC and the Canada Research Chairs' program. GAA thanks the Department of Physical Chemistry (Uppsala) for its hospitality, and Profs. T. Carrington, J. Gao and D. Truhlar for discussions.

References

[1] D.C. Jacobs, Nature 423 (2003) 488.
[2] B.C. Stipe, M.A. Rezaei and W. Ho, Science 280 (1998) 1732.
[3] J.I. Pascual, N. Lorente, Z. Song, H. Conrad and H.-P. Rust, Nature 423 (2003) 525.
[4] S.-W. Hla, L. Bartels, G. Meyer and K.-H. Rieder, Phys. Rev. Lett. 85 (2000) 2777.
[5] H. Park, J. Park, A.K.L. Lim, E.H. Anderson, A.P. Alivisatos and P.L. McEuen, Nature 407 (2000) 57.
[6] S.J. Benkovic and S. Hammes-Schiffer, Science 301 (2003) 1196.
[7] (a) M. Born and K. Huang, *Dynamical Theory of Crystal Lattices* (Clarendon, Oxford, 1954); (b) A.A. Kiselev, J. Phys. B 3 (1970) 904.
[8] B.T. Sutcliffe, in: *Potential Energy Surfaces*, eds. A.F. Sax (Springer, Berlin, 1999).
[9] L.J. Butler, Annu. Rev. Phys. Chem. 49 (1998) 125.
[10] J.C. Tully, In: *Modern Methods for Multidimensional Dynamics Computations in Chemistry*, eds. ed. D.L. Thompson (World Scientific, Singapore, 1998).
[11] H. Nakamura and D. Truhlar, J. Chem. Phys. 115 (2001) 10353; *ibid.* 117 (2002) 5576.
[12] (a) O. Tapia, In: *Quantum Systems in Chemistry and Physics*, eds. A. Hernández-Laguna *et al.* Vol. 2 (Kluwer, Dordrecht, 2000); (b) O. Tapia, Adv. Quantum Chem. 40 (2001) 103; (c) O. Tapia and P. Braña, J. Mol. Str.-Theochem 580 (2002) 9.
[13] (a) T. Kato, Trans. Am. Math. Soc. 70 (1951) 195; (b) W.E. Thirring, In: *Schrödinger: Centenary Celebration of a Polymath*, ed. C.W. Kilmister (Cambridge University Press, 1987).
[14] G.A. Arteca, F.M. Fernández and E.A. Castro, *Large-order Perturbation Theory and Summation Methods in Quantum Mechanics* (Springer, Berlin, 1990).

[15] F.T. Smith, Phys. Rev. 179 (1969) 111.
[16] H. Gabriel and K. Taubjerg, Phys. Rev. A 10 (1974) 741.
[17] M. Baer, Chem. Phys. Lett. 35 (1975) 112.
[18] C.A. Mead and D.G. Truhlar, J. Chem. Phys. 77 (1982) 6090.
[19] A. Thiel and H. Köppel, J. Chem. Phys. 110 (1999) 9371.
[20] M. Baer, J. Phys. Chem. A 104 (2000) 3181.
[21] D.R. Yarkony, J. Chem. Phys. 112 (2000) 2111.
[22] M. Baer and A. Alijah, Chem. Phys. Lett. 319 (2000) 489.
[23] B.K. Kendrick, C.A. Mead and D.G. Truhlar, Chem. Phys. Lett. 330 (2000) 629.
[24] M. Baer, Chem. Phys. Lett. 330 (2000) 633.
[25] H. Köppel, In: *Conical Intersection: Electronic Structure, Dynamics, and Spectroscopy*, eds. W. Domcke *et al*. (World Scientific, Singapore, 2004).
[26] G.A. Arteca and O. Tapia, J. Math. Chem. 35 (2004) 1.
[27] U. Galster, U. Müller and H. Helm, Phys. Rev. Lett. 92 (2004) 073002.
[28] (a) A.R. Miller, J. Am. Chem. Soc. 100 (1978) 1984; (b) N. Agmon, J. Chem. Soc. Faraday Trans. II 74 (1978) 388; (c) J.R. Murdoch, J. Am. Chem. Soc. 105 (1983) 2667.
[29] G.A. Arteca and P.G. Mezey, J. Comput. Chem. 9 (1988) 728.
[30] (a) L.A. Clark, D.E. Ellis and R.Q. Snurr, J. Chem. Phys. 114 (2001) 2580; (b) S.C. Ammal, H. Yamataka, M. Aida and M. Dupuis, Science 299 (2003) 1555.
[31] J.C. Tully, J. Chem. Phys. 93 (1990) 1061.
[32] G. Hirsch, R.J. Buenker and C. Petrongolo, Mol. Phys. 70 (1990) 835.
[33] D. Borgis and J.T. Hynes, Chem. Phys. 170 (1993) 315.
[34] (a) S. Hammes-Schiffer and J.C. Tully, J. Chem. Phys. 101 (1994) 4657; *ibid.* 103 (1995) 8528; (b) S.Y. Kim and S. Hammes-Schiffer, J. Chem. Phys. 119 (2003) 4387.
[35] M. Head-Gordon and J.C. Tully, J. Chem. Phys. 103 (1995) 10137.
[36] G.J. Atchity and K. Ruedenberg, Theor. Chem. Acc. 97 (1997) 47.
[37] D. Kohen, F.H. Stillinger and J.C. Tully, J. Chem. Phys. 109 (1998) 4713.
[38] N. Matsunaga and D.R. Yarkony, Mol. Phys. 93 (1998) 79.
[39] (a) R. Kapral and G. Ciccotti, J. Chem. Phys. 110 (1999) 8919; (b) S. Nielsen, R. Kapral and G. Cicotti, J. Chem. Phys. 112 (2000) 6543; (c) R. Kapral, J. Phys. Chem. A 105 (2001) 2885; (d) A. Sergi and R. Kapral, J. Chem. Phys. 118 (2003) 8566; ibid. 119 (2003) 12776.
[40] C. Alhambra, J.C. Corchado, M.L. Sanchez, J. Gao and D.G. Truhlar, J. Am. Chem. Soc. 122 (2000) 8197.
[41] K.F. Wong and P.J. Rossky, J. Chem. Phys. 116 (2002) 8418; *ibid*. 116 (2002) 8429.
[42] E.S. Kryachko and A.J.C. Varandas, Int. J. Quantum Chem. 89 (2002) 255.
[43] F. Thorpe and C. L. Brooks III, J. Phys. Chem. B 107 (2003) 14042.
[44] E. Deumens, A. Diz, R. Longo and Y. Öhrn, Rev. Mod. Phys. 66 (1994) 917.
[45] N.L. Doltsinis, In: *Quantum Simulations of Complex Many-Body Systems: From Theory to Algorithms*, eds. J. Grotendorst *et al*. NIC Series, Vol. 10 (J. von Neumann Institute for Computing, Jülich, 2002).